DOI: 10.6060/ivkkt.20246709.7049

УДК: 542.973:662.75

РЕГУЛИРОВАНИЕ СВОЙСТВ БИФУНКЦИОНАЛЬОГО КОБАЛЬТОВОГО КАТАЛИЗАТОРА СИНТЕЗА ФИШЕРА-ТРОПША ПРИ ИСПОЛЬЗОВАНИИ ИЕРАРХИЧЕСКОГО ЦЕОЛИТА HBETA

О.П. Папета, В.Г. Бакун, И.Н. Зубков, А.Н. Салиев, А.П. Савостьянов, Р.Е. Яковенко

Ольга Павловна Папета (ORCID 0000-0002-7334-1821), Вера Григорьевна Бакун (ORCID 0000-0002-0971-8145), Иван Николаевич Зубков (ORCID 0000-0003-0828-3159), Алексей Николаевич Салиев (ORCID 0000-0002-5787-3393), Александр Петрович Савостьянов (ORCID 0000-0002-5349-2443), Роман Евгеньевич Яковенко (ORCID 0000-0001-9137-7265)*

НИИ «Нанотехнологии и новые материалы», Южно-Российский государственный политехнический университет им. М.И. Платова, ул. Просвещения, 132, Новочеркасск, Российская Федерация, 346428
E-mail: olya.papeta@mail.ru, b23195@mail.ru, 71650021.qwe@mail.ru, saliev.aleksei@yandex.ru, savostap@mail.ru, jakovenko39@gmail.com*

В данной работе синтезированы новые бифункциональные кобальтовые катализаторы для синтеза Фишера-Тропша в виде композитной смеси: металлического компонента - катализатора Co-Al_2O_3/SiO_2, кислотного компонента - цеолита HBeta и бемитового связующего - AlO(OH). В цеолите HBeta (с мольным соотношением SiO_2/Al_2O_3 40,5) в протонной форме пористая структура была оптимизирована щелочной обработкой (молярная концентрация NaOH: 0,1, 0,15, 0,25, 0,3 и 0,5) с целью получения максимального выхода разветвленных парафинов и олефинов в углеводородах топливного ряда. Катализаторы характеризовались методами рентгенофазового анализа (РФА), низкотемпературной адсорбции-десорбции N_2 и температурно-программированного восстановления водородом (ТПВ H_2), образца цеолита- энергодисперсионного микроанализа поверхности (ЭДА), термогравиметрии (ТГА), сканирующей электронной микроскопии (СЭМ) и адсорбции-десорбции N_2. Оценена эффективность обработки раствором NaOH на развитие мезопористости структуры HBeta. Исследования по синтезу Фишера-Тропша со стационарным слоем катализатора проводились при давлении 2 МПа, температуре 240 – 250 °С и объемной скорости газа 1000 $ч^{-1}$. Балансовые опыты проводили в течение 70-80 ч, анализируя каждые 2 ч состав и количество газа на выходе установки. Показано, что повышение температуры синтеза с 240 до 250 °С интенсифицирует процесс синтеза – степень конверсии CO-катализаторов увеличивается на 9-12%. Проанализирован состав продуктов синтеза Фишера-Тропша. Установлено, что селективность по образованию углеводородов в топливных фракциях, с высокой степенью изомеризации и производительность катализаторов обеспечиваются применением HBeta, модифицированного раствором NaOH с концентрацией 0,25 и 0,5 М.

Ключевые слова: синтез Фишера-Тропша, бифункциональный кобальтовый катализатор, иерархический цеолит HBeta, щелочное модифицирование, мезопористость, селективность

REGULATION OF PROPERTIES OF A BIFUNCTIONAL COBALT CATALYST FOR FISCHER-TROPSCH SYNTHESIS USING HIERARCHICAL HBETA ZEOLITE

O.P. Papeta, V.G. Bakun, I.N. Zubkov, A.N. Saliev, A.P. Savost'yanov, R.E. Yakovenko

Ol'ga P. Papeta (ORCID 0000-0002-7334-1821), Vera G. Bakun (ORCID 0000-0002-0971-8145), Ivan N. Zubkov (ORCID 0000-0003-0828-3159), Aleksey N. Saliev (ORCID 0000-0002-5787-3393), Alexander P. Savost'yanov (ORCID 0000-0002-5349-2443), Roman E. Yakovenko (ORCID 0000-0001-9137-7265)*

Research Institute «Nanotechnologies and New Materials», Platov South-Russian State Polytechnic University (NPI), Prosveschenya st., 132, Novocherkassk, 346428, Russia
E-mail: olya.papeta@mail.ru, b23195@mail.ru, 71650021.qwe@mail.ru, saliev.aleksei@yandex.ru, savostap@mail.ru, jakovenko39@gmail.com*

In this work, new bifunctional cobalt catalysts for Fischer-Tropsch synthesis were synthesized in the form of a composite mixture: a metal component - the Co-Al_2O_3/SiO_2 catalyst, an acid component - HBeta zeolite and a boehmite binder - AlO(OH). In HBeta zeolite (with SiO_2/Al_2O_3 molar ratios of 40.5) in protic form, the porous structure has been optimized with an alkaline treatment (molar NaOH concentration: 0.1, 0.15, 0.25, 0.3 and 0.5) to ensure the production of branched paraffins and olefins in fuel hydrocarbons. The catalysts are characterized by X-ray diffraction (XRD), low-temperature N2 adsorption-desorption and temperature-programmed hydrogen reduction (TPR H_2), zeolite-energy dispersive surface microanalysis (EDM), thermogravimetry (TGA), scanning microscopy (SEM) and adsorption-desorption of N_2. The effectiveness of treatment with NaOH solution to increase the mesoporosity of the HBeta structure was assessed. Research on Fischer-Tropsch synthesis was carried out with a stationary catalyst bed at a pressure of 2 MPa, a temperature of 240 – 250 °C and a gas velocity of 1000 h^{-1}. Balance experiments were carried out for 70–80 h, analyzing the composition and amount of gas at the outlet. It has been shown that increasing the synthesis temperature from 240 to 250 °C intensifies the synthesis process - the degree of conversion of CO catalysts increases by 9-12%. The composition of the Fischer-Tropsch synthesis products was analyzed. It has been established that selectivity of the formation of hydrocarbons in fuel fractions, with a high degree of isomerization and catalyst productivity, determines with the use of HBeta, a modified by NaOH solution with a concentration of 0.25 and 0.5 M.

Key words: Fischer-Tropsch synthesis, bifunctional cobalt catalyst, hierarchical HBeta zeolite, alkali modification, mesoporosity, selectivity

Для цитирования:
Папета О.П., Бакун В.Г., Зубков И.Н., Салиев А.Н., Савостьянов А.П., Яковенко Р.Е. Регулирование свойств бифункционального кобальтового катализатора синтеза Фишера-Тропша при использовании иерархического цеолита HBeta. *Изв. вузов. Химия и хим. технология*. 2024. Т. 67. Вып. 9. С. 62–75. DOI: 10.6060/ivkkt.20246709.7049.

For citation:
Papeta O.P., Bakun V.G., Zubkov I.N., Saliev A.N., Savost'yanov A.P., Yakovenko R.E. Regulation of properties of a bifunctional cobalt catalyst for Fischer-Tropsch synthesis using hierarchical HBeta zeolite. *ChemChemTech [Izv. Vyssh. Uchebn. Zaved. Khim. Khim. Tekhnol.]*. 2024. V. 67. N 9. P. 62–75. DOI: 10.6060/ivkkt.20246709.7049.

INTRODUCTION

The study of GTL processes using an integrated technology that combines the synthesis of hydrocarbons using the Fischer-Tropsch method from CO and H_2 (FT) and the processing of the resulting products [1-3], has been especially relevant recently for the production of high-quality environmentally friendly (green fuel) [1, 4]. Implementation of such technology requires the use of a highly active catalyst capable of operating under the conditions of limited diffusion of synthesized bulk molecules to the acid sites of the catalyst and removal of secondary reaction products [5], when the external surface of the catalyst is involved in the process and the internal surface of the catalyst remains unused [6-8], and the products do not reach the active centers inside some of the pores and channels of the zeolite, which is necessary for hydrocracking and isomerization [9]. As a consequence, mass transfer, rate and efficiency of the process are limited, causing carbonization and accelerating catalyst deactivation [5].

A significant part of these problems is solved by developing new multifunctional FT catalysts. For the selective production of hydrocarbons from fuel fractions, we proposed a composite catalytic system [10-12], containing a metal component - a catalyst for the synthesis of FT Co-Al_2O_3/SiO_2 for the synthesis of long-chain hydrocarbons [13], and an acid component - zeolite of the pentasil group ZSM-5 in H -form. A tested system in the form of a granular mixture of components, by changing the type and topology of the zeolite component, allows you to adjust the acidic properties and structure of the catalyst, thereby controlling the efficiency of the synthesis and solving problems associated with steric restrictions caused by the microporous structure of zeolites. The latter, in particular, can be removed with the development of mesopores (2-50 nm) and the creation of a hierarchical zeolite structure with a bimodal micro-mesoporous pore size distribution [13]. The resulting mesopores (heterogeneous and disordered [5, 14]) can be associated with the outer surface of the zeolite, be isolated in the crystal structure, be associated with micropores [15, 16], facilitating the transfer of large molecules, reducing the path

length inside zeolite particles and crystals, and intensifying the synthesis of FT in general [6]. It is important that to achieve optimal selectivity for target fuel products, the catalytic functions of the system can be tuned separately [17, 18].

While creating the hierarchical structures, when the system of micropores is complemented by secondary mesoporosity [19], the process of rearrangement of zeolite structure is usually divided into two categories [15, 20, 21-24]: formation during synthesis (bottom-up approach) and through postsynthetic processing (top-down approach) [17, 25, 26]. In the first case, template methods are used (using one or more templates), in the second - non-template methods (by selective removal of atoms of the zeolite framework and the creation of intracrystalline mesopores) [21], with hydrothermal [17, 26, 27], acid (dealuminization) [18, 28-30] and/or alkaline treatment (desiliconization [24, 25, 31-34]). Modification is in demand for optimizing selectivity in many acid-catalyzed processes, including variants of FT synthesis [1, 34, 35], especially for the direct conversion of synthesis gas into hydrocarbons with a certain number of carbon atoms and a branched structure [17, 35].

Post-synthesis by alkaline modification, based on the removal of silicon from the zeolite framework, has been well studied for MFI-type zeolites, especially for ZSM-5 [5, 26, 34] and for zeolites of different topologies conforming the versatility of this process [6-8]. Of the MFI, BEA, FER and MOR zeolites currently used in practice, the BEA type is most susceptible and promising for the development of a hierarchical structure to the effects of alkali (usually NaOH) - the disordered structure and small crystallites favor high activity [14, 33, 36], for example, HBeta zeolite for obtaining middle distillates [37]. This tendency of Beta zeolites to alkaline modification is mainly due to the structure of the zeolite rings and the low stability of aluminum in the zeolite framework [15, 38]. Note that during post-synthesis using NaOH solution as a modifying agent, among the process parameters (solution concentration, temperature, time), the only significant variable for the development of mesoporosity is concentration [33].

Most of the studies in the field of bifunctional cobalt catalysts with a hierarchical zeolite structure for Fischer-Tropsch synthesis are devoted to catalysts prepared by the impregnation method [1]. Impregnating catalysts are made by applying a solution of a precursor (mainly an inorganic salt) to the surface of a porous carrier. The disadvantage of such catalysts is the strong interaction of metal cations with a negatively charged zeolite surface. This leads to poor recoverability of the active component and slightly reduces the conversion of CO [1, 9].

In our work we propose composite bifunctional catalysts with hierarchical structure of Beta zeolite prepared by physical mixing of cobalt catalyst (Co-Al_2O_3/SiO_2), an acidic component (hierarchical Beta zeolite) and binder (boehmite). The advantage of such catalysts is that cobalt is not applied to zeolite, which causes a better recoverability of the metal component. The use of bemite as a binder makes it possible to obtain granular catalytic systems that can be used in industrial processes, and the presence of hierarchical Beta zeolite will reduce the diffusion limitations and increase the efficiency of the catalyst [29, 30, 39]. It is important to note that there is practically no work in the field of bifunctional composite hybrid catalysts prepared by mechanical mixing. Therefore, there are no unambiguous ideas about how the use of hierarchical Beta zeolite in the proposed catalytic system will affect the catalytic activity and composition of the resulting Fischer-Tropsch synthesis products.

The aim of this work was to investigate the effect of hierarchical Beta zeolite obtained by post-synthetic alkali treatment on the catalytic activity of the composite bifunctional catalyst and product composition in Fischer-Tropsch synthesis.

EXPERIMENTAL

For the studies, we used synthetic Beta zeolite powder (size 100 μm) of the BEA type with a molar ratio of SiO_2/Al_2O_3 equal to 40.5 in proton form, obtained by calcination of the ammonia form of the zeolite (Zeolyst International) for 6 h at a temperature of 550 °C (initial). To prepare modified samples, a 10 g sample of zeolite was transferred to a beaker, after which 100 ml of NaOH solution with a concentration of, M: 0.1, 0.15, 0.25, 0.3 and 0.5. The treatment was carried out on an electric oven with a magnetic stirrer for 1 h at a temperature of 70 °C. After this by washing with distilled water at room temperature and drying them for 8 h at a temperature of 100-120 °C after which they were calcined for 3 h at 300 °C. The H-form of the samples was obtained by treating with a solution of NH_4NO_3 with a concentration of 1 M for 1 h at a temperature of 70 °C, after which they were dried for 8 h at a temperature of 100-120 °C and calcined for 6 h at 550 °C. Zeolite samples were designated: original - C, modified - x C, where x is the concentration of the NaOH solution used in the treatment, 0.1, 0.15, 0.25, 0.3 and 0.5 M.

Bifunctional cobalt catalysts for the synthesis of FT were obtained in the form of a composite mixture of components. As a metal component of the composi-

tion, a Co-Al_2O_3/SiO_2 catalyst was used for the selective synthesis of long-chain hydrocarbons [40-44] with a silica gel carrier KSKG (Salavat Catalyst Plant LLC), acid - original or modified HBeta zeolite, binder - boehmite (Sasol, TH 80) [12].

The catalysts were prepared by mixing powders (fraction <0.1 mm), wt.%: Co-Al_2O_3/SiO_2 catalyst – 35, HBeta zeolite – 30, boehmite – 35 [43-45]. To plasticize the boehmite binder, an aqueous-alcohol solution of nitric acid and triethylene glycol was used (HNO_3 solution was prepared by adding 1-2 ml of acid with a concentration of 65% by weight in 90-100 ml of distilled water per 100 g of powder mixture, $C_6H_{14}O_4$ was introduced based on the volume ratio of HNO_3: $C_6H_{14}O_4$ in a 1:3 mixture). The catalyst granules were formed by extrusion and were further dried for 24 h at room temperature, 4-6 h at a temperature of 80-100 °C, 2-4 h at a temperature of 100-150 °C and calcined for 5 h at a temperature of 400 °C. The catalysts were designated: original - K, with modified zeolite - x K, where x is the concentration of the NaOH solution: 0.1, 0.15, 0.25, 0.3 and 0.5 M.

Energy dispersive microanalysis of the surface (EDM) was carried out on a Quanta 200 scanning electron microscope (FEI, USA) at an accelerating voltage of up to 30 kV. The surface morphology of zeolites was studied by scanning electron microscopy (SEM) using a JSM-6490LV microscope (JEOL, Japan).

The cobalt content in the catalysts was determined by X-ray fluorescence analysis on an ARL QUANT'X X-ray energy dispersive spectrometer (Thermo Scientific, USA) under the following conditions: medium – air, Teflon substrate, effective irradiation area 48.9 mm^2.

X-ray phase analysis (XRD) of zeolites and catalysts was carried out using a Thermo Scientific ARLX'TRA Powder Diffractometer (Thermo Fisher Scientific, Switzerland) with CuK1,2 radiation using the point-by-point scanning method (step 0.02°, accumulation time at a point 1 s) in the range 2θ 5°-90°. Identification of the phase composition was carried out using the ICDD PDF-2 electronic database of diffraction standards in the Crystallographica software package. The calculation of the relative degree of crystallinity of zeolites was carried out taking into account the integral intensity of characteristic reflections in the 2θ range of 20°-24° [45]. The original sample with a degree of crystallinity of 94% was used as a standard. X-ray diffraction patterns were processed in the FullProf program, the average particle size of cobalt oxide for the characteristic line with a 2θ value of 36.8° was calculated using the Scherrer equation [46], and the average particle size and dispersity of metallic cobalt were calculated in accordance with [47, 48].

The study of the parameters of the porous structure of zeolites and catalysts was carried out by the nitrogen adsorption-desorption method using a Nova 1200e sorbometer gas sorption analyzer (Quantachrome, USA) [39, 42]. The specific surface area was calculated using the BET (Brunauer-Emmett-Teller) method at a relative partial gas pressure P/P_0 = = 0.20. The pore volume was determined by the BJH method at a relative partial pressure P/P_0 = 0.95, the pore size distribution was calculated from the BJH desorption curve (Barrett-Joyner-Halenda), the volume of micropores in the presence of mesopores was measured using the t-method (de Boer and Lippens). Previously, the samples were subjected to vacuum treatment for 5 h at a temperature of 350 °C. The volume of meso- and macropores was calculated using the instrument software package.

Thermogravimetric analysis (TGA) of zeolites was performed using an STA 449 F5 simultaneous thermal analysis device combined with a QMS Aeolos Quadro mass spectrometer (Netzsch, Germany). The zeolites were first dried for 1 h at a temperature of 150 °C. The survey was carried out under the following conditions: inert medium (helium 70 min^{-1}), sample weight 30 mg, temperature range 50-1000 °C, heating rate 20 °C min^{-1}.

The catalysts were studied by temperature-programmed reduction with hydrogen (H_2 TPR) using a Micromeritics ChemiSorb 2750 analyzer (Micromeritics, USA). with thermal conductivity detector (TCD). The catalysts were preliminarily kept in a helium flow (20 ml min^{-1}) for 1 h at a temperature of 200 °C. Then it was cooled to room temperature and a mixture of 10% hydrogen and 90% nitrogen (20 ml min^{-1}) was supplied. The studies were carried out in the temperature range 20-800 °C with a heating rate of 20 °C min^{-1}.

The study of the catalytic properties in the synthesis of FT was carried out in an isothermal reactor with a diameter of 16 mm with a stationary catalyst bed. 5-10 cm^3 of catalyst (1-2 mm fraction) mixed with 15-30 cm^3 of quartz was loaded into the reactor. The catalyst was reduced with hydrogen for 1 h at a temperature of 400 °C and a gas space velocity of 3000 h^{-1}. Activation of samples with synthesis gas with a ratio H_2/CO = 2 and catalytic tests were carried out at a pressure of 2.0 MPa and a gas volumetric velocity of 1000 h^{-1}, raising the temperature from 180 °C to 230-250 °C at a rate of 2.5 °C h^{-1}. Balance experiments were carried out for 70-80 h, analyzing the composition and amount of gas at the outlet of the installation every 2 h. The activity of the catalysts was judged by the conversion of CO, the selectivity and productivity of the catalysts, and the fractional and hydrocarbon composition of the synthesis products.

Analysis of the composition of the source gas and gaseous synthesis products was carried out using a Crystal 5000 gas chromatograph (Khromatek, Russia), equipped with a thermal conductivity detector and two columns (Haysep R active phase and NaX molecular sieves). The analysis mode is temperature-programmable with a heating rate of 8 °C min^{-1}. The condensed products were separated by distillation at atmospheric pressure, isolating fuel fractions with boiling points: gasoline - up to 180 °C, diesel - 180-330 °C, residue - above 330 °C. The composition of C_{5+} hydrocarbons was determined using an Agilent 7890A chromatography-mass spectrometer (Agilent Technologies, USA) equipped with an MSD 5975C detector (Agilent, USA) and an HP-5MS capillary column.

RESULTS AND DISCUSSION

According to local elemental analysis (EDA), an increase in aluminum content and a decrease in the Si/Al molar ratio in the HBeta structure as a result of treatment with a NaOH solution is recorded at a modifier concentration of 0.25-0.5 M (Table 1). The extraction of silicon atoms from the zeolite framework occurs predominantly from the outside of the crystals [25] from a three-dimensional crystal structure formed by the junction of neutrally charged TO4 tetrahedra (T = = Si, Al) bound by oxygen atoms with partial isomorphic replacement of Si^{4+} by Al^{3+} [13, 18, 23, 45, 46]. The degree of silicon extraction for the 0.3 Z sample is 2.3%, for the 0.5 Z sample it is already 17.3%. It is obvious that the effect of NaOH, as a strong modifier [32], causes the leaching of silicon atoms, causing partial destruction and then amorphization of the HBeta structure [25, 33]. The process may be accompanied by the extraction of small amounts of aluminum (the main part is capable of realuminization) [35, 44]. As a result, a decrease in the Si/Al ratio causes the appearance of a negative charge on AlO_4 (-1) tetrahedra [14, 19] and, due to the repulsion of charges and ions of the OH^- solution, prevents the extraction of silicon atoms [22, 49] – hydrolysis of the Si-O- Al bond is difficult, in comparison with the relatively easy cleavage of the Si-O-Si bond in the absence of AlO_4 groups in the immediate environment [37, 50-53].

Table 1

Elemental composition of the surface of zeolites

***Таблица 1.* Элементный состав поверхности цеолитов**

Zeolite	Content, %		Si/Al ratio	Degree of extraction Si, %
	Si	Al		
Z	40.0	3.0	13.3	-
0.25 Z	39.0	3.0	13.0	2.3
0.3 Z	40.4	3.1	13.0	2.3
0.5 Z	39.8	3.6	11.0	17.3

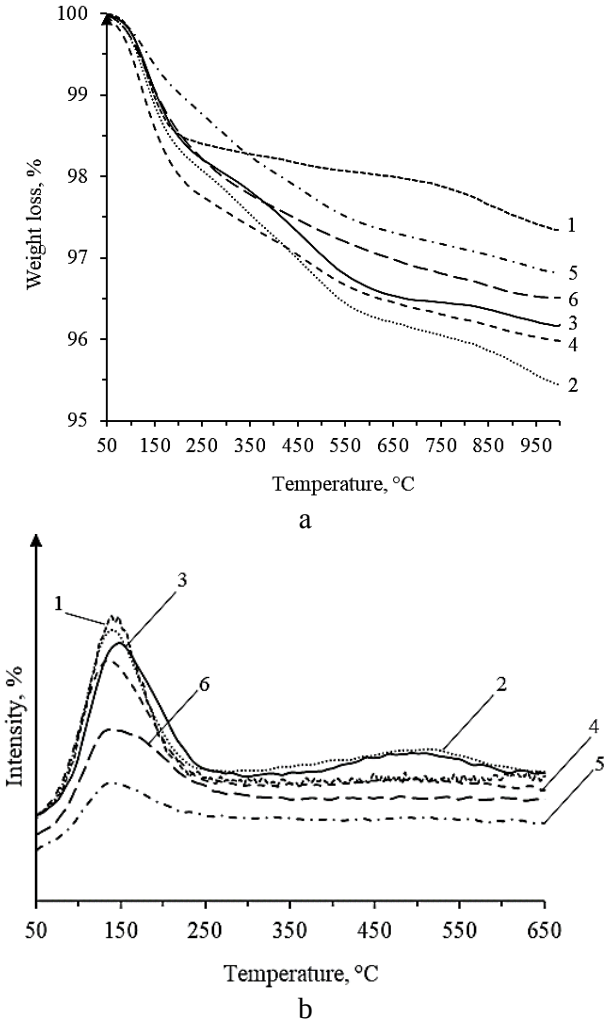

Fig. 1. Thermogravimetric curves of mass loss (a) and water release for (b) zeolites: Z (1), 0.1 Z (2), 0.15 Z (3), 0.25 Z (4), 0.3 Z (5), 0.5 Z (6)

Рис. 1. Термогравиметрические кривые потери массы (a) и выделения воды для цеолитов (b): Z (1), 0,1 Z (2), 0,15 Z (3), 0,25 Z (4), 0,3 Z (5), 0,5 З (6)

The Si/Al ratio determines the amount of moisture bound in the crystal structure of the zeolite, since to compensate for the excess negative charge of the tetrahedra outside the frame, channels and cavities of molecular sizes are occupied by cations of hydrogen, alkali or alkaline earth metals and water molecules [14, 19]). The processes of moisture loss in the temperature range 50-1000 °C, occurring in the volume and on the surface of air-dry zeolite samples, associated with the level of transformation of the HBeta crystal structure, are illustrated in Fig. 1. The nature of the dependences of weight loss (a) and moisture release (b), with the exception of curves for HBeta zeolite (1 in Fig. 1 a) and samples treated with NaOH solution with concentrations of 0.1 and 0.15 M (2 and 3 in Fig. 1 b), as well as the number of thermal effects, are the same. The processes occur gradually, with a loss of 2.7-4.6% of

mass. The smallest moisture losses correspond to samples 0.3 Z and 0.5 Z; for other samples they are close, but the release occurs at different rates. Thus, a high aluminum content in the structure of zeolites stimulates hydrophilicity, while a lower aluminum content stimulates hydrophobicity [54, 55]. Desorption of moisture adsorbed from the environment and physically bound to the zeolite surface is observed in the temperature range of 100-200 ℃. For samples 0.1 Z and 0.15 Z with the structure least affected by treatment, the release of the second type of moisture is observed in the region of 300-600 ℃ - intra-crystallization.

A comparison of the crystal structure of the original and modified HBeta samples was carried out by X-ray diffraction. It was determined [41] that the main reflections of zeolite in the region of 2θ angles of 7.7°, 21.3° and 22.4° [56] are identical to the Beta phase (000-056-0467) (Fig. 2) [28, 16, 18], including 7.7° and 22.4° – correspond to polymorphic modifications A and B of zeolite [16]. In accordance with the topology of the framework [57, 58], the Beta crystal lattice is mainly represented by 12-membered rings [59], formed by the intergrowth [14] of these modifications of tetragonal and monoclinic symmetry, which causes the appearance of a large number of surface and volumetric stacking faults. The noted increase in the intensity of the 7.7° reflection for samples 0.1 Z and 0.15 Z may be caused by an increase in their number [37]. Treatment with a NaOH solution with a concentration of 0.25-0.5 M leads to amorphization of the zeolite framework: the intensity and sharpness of the 7.7° and 22.4° reflections decrease [32], in addition, for samples of 0.3 Z and 0.5 Z, the appearance of a diffuse halo and the disappearance of the 21.3° reflection are observed [22, 26]. The assessment of crystallinity (the geometry of the structure associated with the ordering of aluminosilicate tetrahedra of zeolite [38]) confirms the partial amorphization of the structure of the samples [33] (Fig. 2). The degree of crystallinity gradually decreases (from 98 to 45%) for the 0.3 Z sample, then the rate of the process decreases. The significant loss of crystallinity, in comparison with MFI and MOR type structures [37], at high concentrations of NaOH solution according to [22, 26] may be due to the high defectivity and lower stability of aluminum in the HBeta structure [16, 60-62].

The dynamics of the framework restructuring process and the development of HBeta mesoporosity were observed by comparing the surface state and particle geometry of the samples using microstructural analysis (SEM). Based on the shape and orientation of the particles, the zeolite surface has a distinct granular structure (Fig. 3). The initial zeolite consists of clusters of polycrystals of spheroidal morphology, mainly up to 900 nm in size, consisting of many primary nanosized particles of a similar shape with a diameter of 30 nm (Fig. 3a). Clusters of particles are dispersed over the surface and separated by interparticle voids, complementing the system of micropores and forming a volume of secondary pore space [19]. As can be seen from the example of a 0.25 Z sample, when treated with a NaOH solution, the observed nanoparticles decrease to 20-100 nm (Fig. 3 b). The leaching of silicon from the zeolite framework occurs most intensively due to the destruction of small nanoparticles followed by intercrystalline aggregation of structural elements (amorphous aluminosilicate fragments located in mesopores). As a consequence, the proportion of large particles with a size of 400-800 nm and the number and volume of interparticle voids increase. As the concentration of the modifier solution increases to 0.5 M, the structure of the aggregates becomes more amorphous, particles larger than 400-1000 nm dominate, the number of visible relatively small nanoparticles is minimal (Fig. 3c), and the size of developing pores increases.

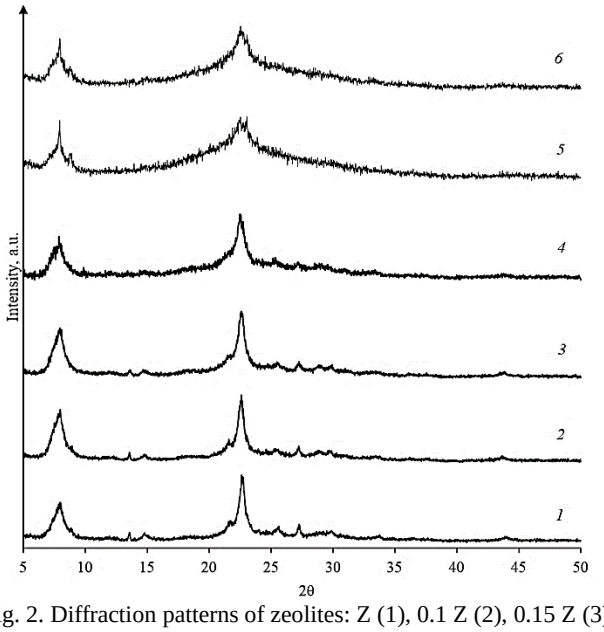

Fig. 2. Diffraction patterns of zeolites: Z (1), 0.1 Z (2), 0.15 Z (3), 0.25 Z (4), 0.3 Z (5), 0.5 Z (6)
Рис. 2. Дифрактограммы цеолитов: Z (1), Z 0,1 (2), Z 0,15 (3), Z 0,25 (4), Z 0,3 (5), Z 0,5 (6)

According to the assessment of changes in the porous structure of the original HBeta and samples with a high degree of transformation of the crystalline framework using the N_2 adsorption-desorption method according to the type of isotherms [35], post synthesis by alkaline treatment is an effective method for the formation of a hierarchical structure of zeolite. With a gradual doubling of the modifier concentration, as can

be seen in the examples of samples 0.25 Z and 0.5 Z, the development of mesoporosity leads to a decrease in the number and volume of micropores V_{micro} from 0.17 cm^3/g by almost 2 and 4 times, the share of V_{micro} in the total pore volume V_Σ 0.37 cm^3/g by 23 and 35%, as a result, the surface area SBET 576 m^2/g by 35 and 43% with a noticeable reduction in external SEX 251 m^2/g by 15% and V_Σ by 2.5% for the 0.25 Z sample, and an increase in SEX and V_Σ for sample 0.5 Z by 3 and 11%.

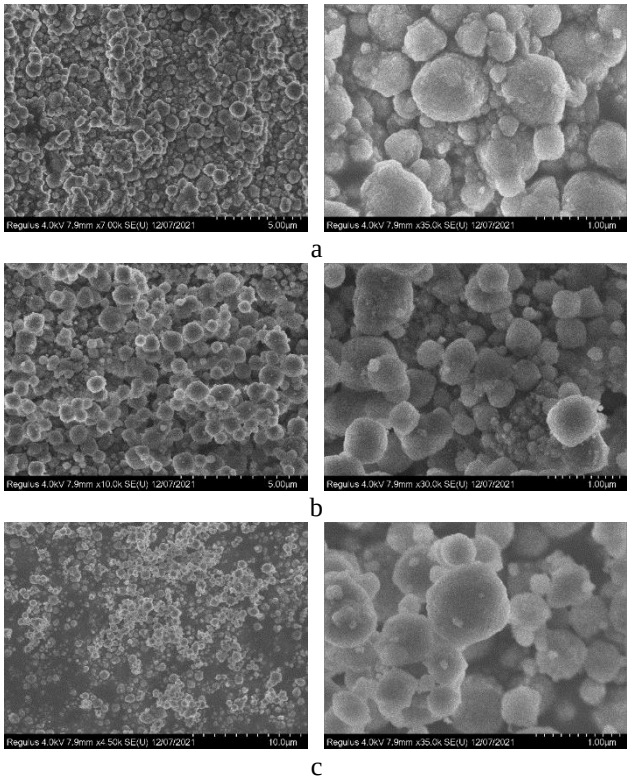

Fig. 3. SEM – images of the surface of zeolites: Z (a), 0.25 Z (b), 0.5 Z (c)

Рис. 3. СЭМ – изображения поверхности цеолитов: Z (a), 0,25 Z (b), 0,5 Z (c)

The formation of bidispersity (micro-mesoporous) structure of the samples is illustrated in Fig. 4. For polymorphic modifications a and b of Beta zeolite, the intersecting linear (ring) channels of the frame have large pores with sizes of 0.73×0.60 nm and 0.73×0.68 nm, tortuous (elliptical cross-section) - 0.56×0.56 nm and 0.55×0.55 nm [6, 14, 16], which is consistent with the data for the original HBeta sample with pores with a pore radius of less than 2 nm (Fig. 4 a). The extraction of silicon from the zeolite framework causes the appearance of new mesopores and a second maximum on the pore size distribution curve: in the range of 2-4 nm for a sample of 0.25 Z and a wider one - 2-6 nm, for a sample of 0.5 Z (Fig. 4 b, c). This type of change in the structure of zeolites during alkaline modification was observed, for example, in [61, 62, 16].

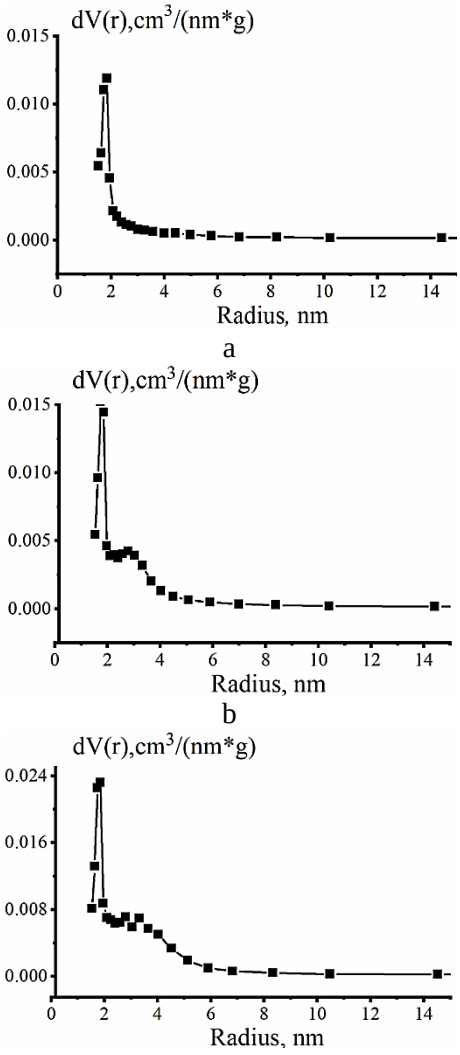

Fig. 4. Pore size distribution for zeolites: Z (a), 0.25 Z (b), 0.5 Z (c)

Рис. 4. Распределение пор по размерам для цеолитов: Z (a), 0,25 Z (b), 0,5 Z (c)

When studying the phase composition of bifunctional catalysts (XRD), it was determined that in terms of the zeolite component, the diffraction patterns of the HBeta samples and catalysts are identical, although the reflections of the zeolite in the mixture of catalyst components are less intense (Fig. 5). The aluminum oxide phase, formed during the thermal decomposition of the boehmite binder, is weakly crystallized and has reflections in the 2θ angle range of 47-70°. The metal component of the catalysts, the concentration of which, according to the results of X-ray fluorescence analysis, is 7.4-7.5%, in the form of Co_3O_4 oxide with a cubic spinel structure of the Fd3m type [40, 41], is fixed on the surface of the Co-$Al2O_3/SiO_2$ catalyst

(SiO_2 is X-ray amorphous). As the crystallinity of the zeolite component framework decreases, the intensity of the main reflections of Co_3O_4 increases, and the size of oxide and metallic cobalt nanoparticles, calculated using the Scherrer equation, changes (Table 2). It can be assumed that as the HBeta structure becomes amorphous, with the appearance and increase in the concentration of aluminum in the pores and on the surface of the zeolite, the possibility for the interaction of cobalt and aluminum compounds, including during the preparation of the catalyst, increases. Thus, after treatment with NaOH solutions with a concentration of 0.1-0.25 M, the average size of Co_3O_4 nanoparticles decreases from 17.5 to 13.0 nm, then at concentrations of 0.3 and 0.5 M, when the particles become larger, it increases to 15.2 nm.

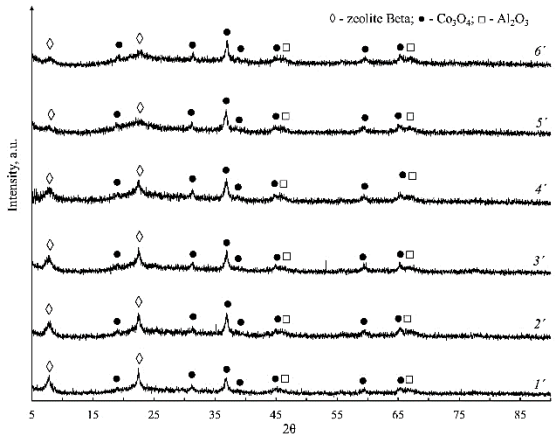

Fig. 5. X-ray diffraction patterns of catalysts: K (1), 0.1 K (2), 0.15 K (3), 0.25 K (4), 0.3 K (5), 0.5 K (6)
Рис. 5. Дифрактограммы катализаторов: K (1), 0,1 K (2), 0,15 K (3), 0,25 K (4), 0,3 K (5), 0,5 K (6)

Table 2

Catalyst parameters according to XRD data
***Таблица 2.* Параметры катализаторов по данным**

Catalyst	Particle size, nm		Dispersity Co^0, %
	Co_3O_4	Co^0	
K	17.5	13.0	7.5
0.1 K	14.1	10.5	9.3
0.15 K	13.1	9.8	10.0
0.25 K	13.0	9.8	10.0
0.3 K	14.4	10.8	9.1
0.5 K	15.2	11.3	8.7

The process of formation of the porous structure of catalysts (including the secondary one) is reflected by the pore size distribution curves in Fig. 5, which make it possible to estimate the spatial position of metal and acid centers for observed pores of 1-15 nm in size and include areas in the region: 1-4 nm with maxima around 2 nm and undivided 3 nm, corresponding to the contribution to the total pore volume of micro- and mesopores zeolite; 3-7 nm with a maximum of about 5 nm for Co-Al_2O_3/SiO_2 (Fig. 5 a) and boehmite (4-6 nm according to [41]). As a result, the properties of catalysts are determined by the parameters of the porous structure of the components and the chosen preparation technique (type and concentration of peptizing agent, conditions of mixing, molding and heat treatment of catalysts [63]). Modification of the zeolite component does not affect the total pore volume V_Σ of catalysts 0.55 cm^3/g, but reduces: the share of micropore volume V_{micro} from 0.04 cm^3/g in the total V_Σ by 7 and 2%; SBET 311 m^2/g by 16 and 29% and external surface SEX 224 m^2/g for sample 0.5 Z by 8%. Thus, the formed polydisperse porous structure of catalysts will increase the accessibility of catalytic active centers for reagent molecules [16]. At the same time, the size of the secondary pore space and the transport pore system can be adjusted by controlling the distance between the metal and acid centers of the catalysts at the nano level due to the binder [63].

The reduction of catalyst oxide Co_3O_4 to the metallic state, according to H_2 TPR data (Table 3), proceeds sequentially in two stages [64, 65] with the following scheme: $Co^{3+} \rightarrow Co^{2+}$ and $Co^{2+} \rightarrow Co^0$. The spectra of catalysts with maximums in the temperature ranges of 315-355 °C and 405-450 °C are identical. The decrease in the temperature of the maxima in the spectra of HBeta samples treated with a NaOH solution with a concentration of 0.15-0.3 M may be associated with the smaller size of Co_3O_4 particles. An increase in the temperature of the maxima to maximum values and peak area for the 0.5 Z sample is associated with the binding of cobalt oxide compounds to the aluminum of the zeolite framework (possibly boehmite) with the formation of a significant amount of surface difficult-to-reduce compounds in the catalyst preparation cycle [63, 65].

The catalysts exhibit high activity in the process of FT synthesis (Fig. 6). Thus, with the consistent development of the hierarchical structure of HBeta samples and changes in the complex properties of the catalysts, the main indicators of the process gradually improve. Catalysts using zeolites obtained by treatment with a NaOH solution with a concentration of 0.25-0.5 M have high levels of CO conversion and productivity with respect to the formation of C_{5+} hydrocarbons, the maximum with minimal gas formation is 0.5 M. Increasing the synthesis temperature from 240 °C to 250 °C intensifies the process synthesis - the degree of CO conversion for samples increases by 9-12%. In this case, the balance of secondary hydro processes for the 0.25 K and 0.3 K catalysts, in contrast to

the K and 0.5 K samples, changes somewhat. At the same time, in terms of the achieved indicators, the catalysts, primarily 0.5 K, are not inferior to the most competitive of the known bifunctional FT catalysts.

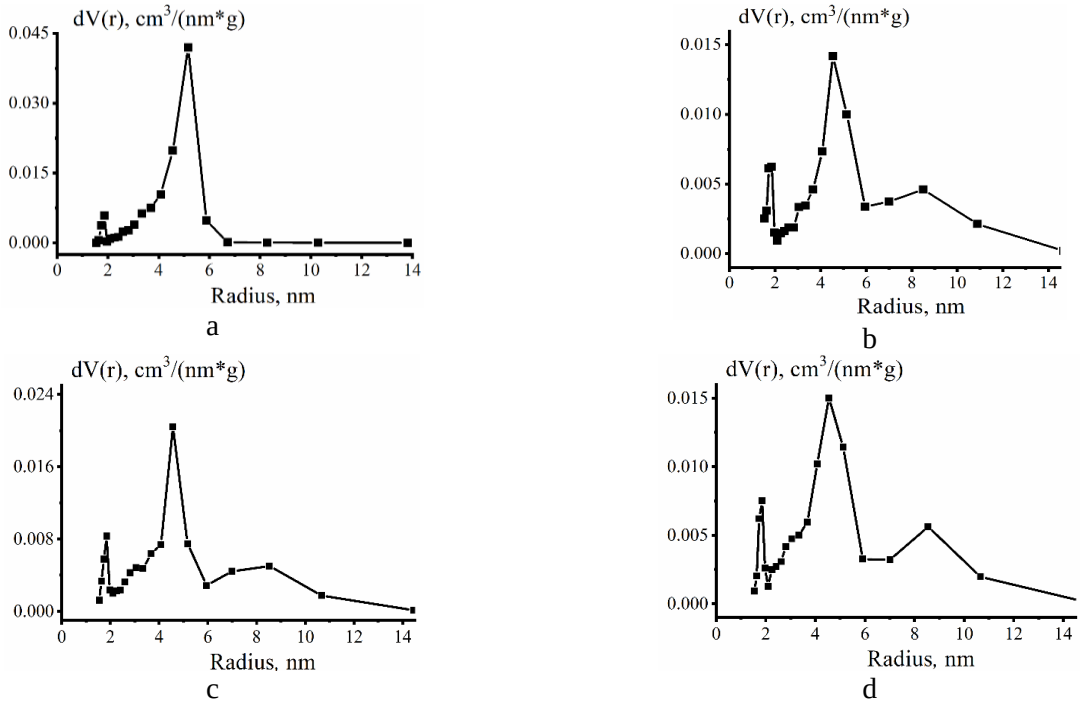

Fig. 6. Pore size distribution for catalysts: Co-Al_2O_3/SiO_2 (a), K (b), 0.25 K (c), 0.5 K (d)
Рис. 6. Распределение пор по размерам для катализаторов: Co-Al_2O_3/SiO_2 (a), K (b), 0,25 K (c), 0,5 K (d)

Table 3

TPR data of H_2 catalysts
***Таблица 3.* Данные ТПВ H_2 катализаторов**

Catalyst	Peak 1		Peak 2	
	Temperature, °C	Square S_1, %	Temperature, °C	Square S_2, %
K	330	29.2	424	70.8
0.1 K	341	28.4	437	71.6
0.15 K	332	26.9	417	73.1
0.25 K	326	27.5	408	72.6
0.3 K	317	27.3	414	72.7
0.5 K	355	25.9	448	74.1

note: S1 and S2 – peak area on the TPR curve
Примечание: S1 и S2 площади пиков ТПВ

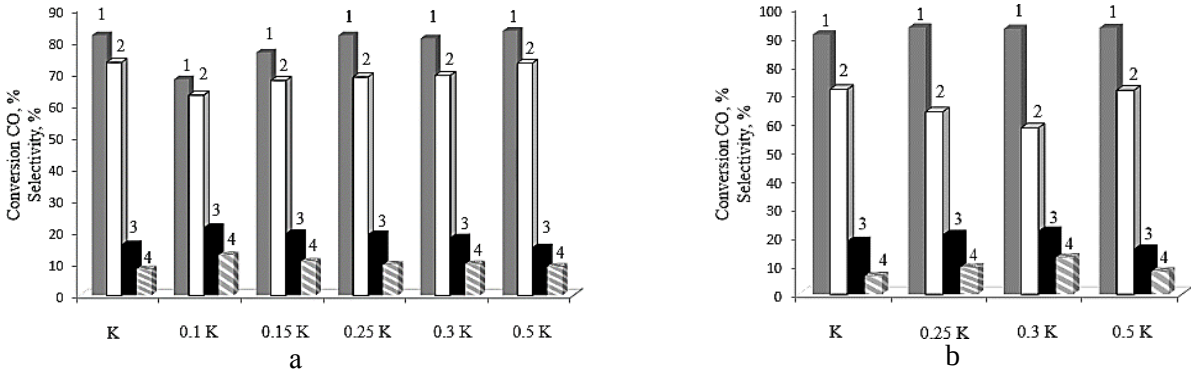

Fig. 7. Catalytic performance of FT synthesis at temperature 240 °C (a) and 250 °C (b) for catalysts: Conversion CO (1), C_{5+} (2), CH_4 (3), C_2-C_4 (4)
Рис. 7. Каталитические показатели синтеза ФТ при температуре 240 °C (a) и 250 °C (b) для катализаторов: Конверсия CO (1), C_{5+} (2), CH_4 (3), C_2-C_4 (4)

C_{5+} hydrocarbons synthesized in the presence of the metal component of catalysts ($Co\text{-}Al_2O_3/SiO_2$) are 97.4% alkanes of normal structure, including 46.7% long-chain C_{19+}. Choosing the optimal method for processing the acid component of catalysts to obtain a given composition of products involves finding a balance between selectivity and activity indicators of the catalytic system in the process of FT synthesis. The data for such an assessment are summarized in table. 6 and allow one to evaluate the functional features of the catalysts. It is obvious that the presence of the acidic component HBeta in the catalyst composition ensures selective hydrocracking and isomerization of primary high-molecular products into hydrocarbons of fuel fractions [61, 19, 27, 66] – mainly alkanes of normal and iso structure, components of gasoline C_5-C_{10} and diesel C_{11}-C_{18} fractions (Table 4). The formation of naphthenic and aromatic hydrocarbons was not recorded.

Table 4

Catalyst performance and composition of C_{5+} hydrocarbons at temperatures of 240 and 250 °C

***Таблица 4.* Производительность катализаторов и показатели состава углеводородов C_{5+} при температурах 240 и 250 °C**

Catalyst	Productivity, kg/(m^3_{cat}·h)					iso/n**	o/p***
	alkanes	alkenes	isoalkanes	alkenes*	total		
240 °C							
K	80.3	18.3	21.8	15.2	135.6	0.4	0.3
0.1 K	52.6	12.5	15.4	12.3	92.8	0.4	0.4
0.15 K	62.7	13.2	21.5	12.7	110.1	0.5	0.3
0.25 K	66.9	12.0	23.2	15.2	117.3	0.5	0.3
0.3 K	75.1	13.9	19.1	12.1	120.2	0.4	0.3
0.5 K	80.2	18.8	22.6	5.1	126.7	0.3	0.2
including C_{11}-C_{18}							
K	39.6	1.3	12.2	2.8	55.9	0.4	0.1
0.25 K	28.0	2.3	13.4	6.0	49.7	0.6	0.2
0.5 K	37.5	4.6	13.9	2.2	58.2	0.4	0.1
250 °C							
K	76.2	20.6	29.3	20.3	146.4	0.5	0.4
0.25 K	62.1	13.4	19.0	29.4	123.9	0.6	0.5
0.3 K	68.3	11.7	17.4	16.0	113.4	0.4	0.3
0.5 K	83.3	17.9	22.7	13.8	137.7	0.4	0.3
including C_{11}-C_{18}							
K	28.5	1.5	17.9	4.4	52.3	0.7	0.1
0.25 K	25.6	2.2	10.5	12.3	50.6	0.8	0.4

*Branched alkenes

**Ratio of hydrocarbons with a branched to linear structure

***The ratio of the content of alkenes (olefins) and alkanes (paraffins)

*Разветвленные алкены

**Соотношение углеводородов с разветвленной и линейной структурой

***Соотношение содержания алкенов (олефинов) и алканов (парафинов)

The transformation of the structure of the zeolite component of 0.1-0.25 K catalysts causes a decrease in the number of n-alkanes in the composition of the synthesis products. In comparison with the catalyst on the original HBeta, for example, at 240 °C there is an increase in the number of n-alkanes in the gasoline fraction and a decrease in the diesel fraction. As changes in the properties of zeolites increase when treated with a modifier in high concentrations (0.25-0.5 M), the balance of cracking and isomerizing functions of catalysts changes – the number of n-alkanes participating in secondary reactions decreases (close results of the influence of the zeolite component on the properties of a composite catalyst are given in the work [61]). Most noticeably for 0.5 K (the total amount of n-alkanes in the diesel fraction increases) – the zeolite promotes the isomerization process without too much cracking [27]. Thus, the formed mesoporous channels ensure the proximity of the reacting molecules, solve the problem of accessibility of active centers and increase the intensity of the isomerization process. In this case, terminal single-branched (monomethyl-branched) alkanes can form inside the pores (close to the entrance to the pore), and double-branched ones - mainly on the outer surface through their isomerization. As a consequence, in the C_{11}–C_{18} fraction of all catalysts with modified HBeta,

hydrocarbons of iso-structure are formed - isoalkanes and branched alkenes, most intensively in the presence of a 0.25 K sample at 240 °C and 250 °C. With a minimum number of normal-structure alkanes formed and a temperature of 240 °C, the proportion of iso-alkanes increases ~ 1.25 times to 27%. The proportion of branched alkenes at 240 °C is 2.4 times to 12%, at 250 °C – 2.9 times to 24%, which together with isoalkanes reaches 45% of the fraction volume. C_{5+} hydrocarbons and components of the diesel fraction obtained in the presence of a catalyst are characterized by maximum values of the iso/n index at all FT synthesis temperatures (0.5 and 0.6, 0.6 and 0.8, respectively).

CONCLUSIONS

The features of the appearance of mesoporosity and the development of bidisperse micro-mesoporous structure of HBeta zeolite samples obtained by post-synthesis during alkaline treatment were studied. The formation of a polydisperse porous structure of composite bifunctional cobalt catalysts for the synthesis of FT using hierarchical HBeta zeolite as an acid component is considered.

It has been shown that optimization of the porous structure of catalysts creates conditions for the selective synthesis of hydrocarbons in fuel fractions. The main parameters that determine the formation of hydrocarbons in gasoline C_5-C_{10} and diesel C_{11}-C_{18} fractions with a high degree of isomerization are the size and nature of the pore size distribution of HBeta zeolite.

It has been established that it is preferable to use HBeta zeolite with a crystalline structure obtained by treatment with a NaOH solution with a concentration of 0.25-0.5 M as an acidic component of catalysts. The productivity of catalysts for C_{5+} hydrocarbons at a synthesis temperature of 250 °C reaches 123.9-137.7 kg $m^{-3}cat \cdot h^{-1}$.

ACKNOWLEDGEMENTS

The work was carried out within the framework of the strategic project "Scientific and Innovation Cluster "Contract R&D Center" of the Development Program of SRSPU (NPI) during the implementation of the strategic academic leadership program «Priority-2030».

The authors declare the absence a conflict of interest warranting disclosure in this article.

Работа выполнена в рамках стратегического проекта «Научно-инновационный кластер «Контрактный научно-исследовательский центр» Программы развития ЮРГПУ (НПИ) в ходе реализации программы стратегического академического лидерства «Приоритет-2030».

Авторы заявляют об отсутствии конфликта интересов, требующего раскрытия в данной статье.

ЛИТЕРАТУРА

1. **Adeleke A.A., Liu X., Lu X., Moyo M., Hildebrandt D.** // *Rev. Chem. Eng.* 2020. V. 36. N 4. P. 437-457. DOI: 10.1515/revce-2018-0012.
2. **Sartipi S.J., Parashar K., Valero-Romero M., Santos V., Linden B., Makkee M., Kapteijn F., Gascon J.** // *J. Catal.* 2013. V. 305. P. 179-190. DOI: 10.1016/j.jcat.2013.05.012.
3. **Асалиева Е.Ю., Синева Л.В., Мордкович В.З.** // *Изв. вузов. Химия и хим. технология.* 2023. Т. 66. Вып. 10. С. 44-51. DOI: 10.6060/ivkkt.20236610.12y.
4. **Arutyunov V.S., Savchenko V.I., Sedov I.V., Nikitin A.V., Troshin K.Y., Borisov A.A., Fokin I.G., Makaryan I.A., Strekova L.N.** // *Eur. Chem.-Technol. J.* 2017. V. 19. N 3. P. 265-271. DOI: 10.18321/ectj662.
5. **Bonetto L., Pierella L.B., Saux C.** // *Bull. Mater. Sci.* 2020. V. 43. N 1. P. 288. DOI: 10.1007/s12034-020-02254-9.
6. **Fernandez S., Ostraat M.L., Zhang K.** // *AIChE J.* 2020. V. 66. N 9. P. e16943. DOI: 10.1002/aic.16943.
7. **Xing C., Yang G., Lu P., Shen W., Gai X., Tan L., Wang T., Yang R., Tsubaki N.** // *Micropor. Mesopor. Mater.* 2016. V. 233. P. 62-69. DOI: 10.1016/j.micromeso.2015.10.021.
8. **Schwanke A.J., Pergher S., Martínez L.M.T., Kharissova O.V., Kharisov B.I.** Hierarchical MWW zeolites by soft and hard template routes. Handbook of Ecomaterials. Switzerland: Springer Nature. 2019. 2537-59. DOI: 10.1007/978-3-319-48281-1_89-1.

REFERENCES

1. **Adeleke A.A., Liu X., Lu X., Moyo M., Hildebrandt D.** // *Rev. Chem. Eng.* 2020. V. 36. N 4. P. 437-457. DOI: 10.1515/revce-2018-0012.
2. **Sartipi S.J., Parashar K., Valero-Romero M., Santos V., Linden B., Makkee M., Kapteijn F., Gascon J.** // *J. Catal.* 2013. V. 305. P. 179-190. DOI: 10.1016/j.jcat.2013.05.012.
3. **Asalieva E.Y., Sineva L.V., Mordkovich V.Z.** // *ChemChemTech [Izv. Vyssh. Uchebn. Zaved. Khim. Khim. Tekhnol.].* 2023. V. 66. N 10. P 44-51 (in Russian). DOI: 10.6060/ivkkt.20236610.12y.
4. **Arutyunov V.S., Savchenko V.I., Sedov I.V., Nikitin A.V., Troshin K.Y., Borisov A.A., Fokin I.G., Makaryan I.A., Strekova L.N.** // *Eur. Chem.-Technol. J.* 2017. V. 19. N 3. P. 265-271. DOI: 10.18321/ectj662.
5. **Bonetto L., Pierella L.B., Saux C.** // *Bull. Mater. Sci.* 2020. V. 43. N 1. P. 288. DOI: 10.1007/s12034-020-02254-9.
6. **Fernandez S., Ostraat M.L., Zhang K.** // *AIChE J.* 2020. V. 66. N 9. P. e16943. DOI: 10.1002/aic.16943.
7. **Xing C., Yang G., Lu P., Shen W., Gai X., Tan L., Wang T., Yang R., Tsubaki N.** // *Micropor. Mesopor. Mater.* 2016. V. 233. P. 62-69. DOI: 10.1016/j.micromeso.2015.10.021.
8. **Schwanke A.J., Pergher S., Martínez L.M.T., Kharissova O.V., Kharisov B.I.** Hierarchical MWW zeolites by soft and hard template routes. Handbook of Ecomaterials. Switzerland: Springer Nature. 2019. 2537-59. DOI: 10.1007/978-3-319-48281-1_89-1.

9. **Sineva L.V., Asalieva E.Y., Mordkovich V.Z.** // *Russ. Chem. Rev.* 2015.V. 84. N 11. P. 1176. DOI: 10.1070/RCR4464.
10. **Савостьянов А.П., Нарочный Г.Б., Яковенко Р.Е., Салиев А.Н., Сулима С.И., Зубков И.Н., Некроенко С.В., Митченко С.А.** // *Нефтехимия*. 2017. Т. 57. Вып. 6. С. 809-812. DOI: 10.7868/S0028242117060326.
11. **Яковенко Р.Е., Зубков И.Н., Бакун В.Г., Аглиуллин М.Р., Салиев А. Н., Савостьянов А.П.** // *Катализ в пром-сти.* 2021. Т. 21. Вып. 1-2. С. 30-40. DOI: 10.18412/1816-0387-2021-1-2-30-40.
12. **Yakovenko R.E., Savost'yanov A.P., Narochniy G.B., Soromotin V.N., Zubkov I.N., Papeta O.P., Svetogorov R.D., Mitchenko S.A.** // *Catal. Sci.Technol.* 2020. V. 10. N 22. P. 7613-7629. DOI: 10.1039/D0CY00975J.
13. **Сулима С.И., Бакун В.Г., Яковенко Р.Е., Шабельская Н.П., Салиев А.Н., Нарочный Г.Б., Савостьянов А.П.** // *Кинетика и катализ.* 2018. Т. 59. Вып. 2. С. 240-250. DOI: 10.7868/S0453881118020132.
14. **Abello S., Bonilla A., Perez-Ramirez J.** // *Appl. Catal. A: Gen.* 2009. V. 364. P. 191-198.
15. **Min J., Kim S., Kwak G., Kim Y.T., Han S.J., Lee Y., Jun K.W., Kim S.K.** // *Catal. Sci. Technol.* 2018. V. 8. N 24. P. 6346-6359. DOI: 10.1039/C8CY01931B.
16. **Tarach K., Góra-Marek K., Tekla J., Brylewska K., Datka J, Mlekodaj K., Makowski W., Igualada López M.C., Triguero J.M., Rey F.** // *J. Catal.* 2014. V. 312. P. 46-57. DOI: 10.1016/j.jcat.2014.01.009.
17. **Li H., Hou B., Wang J., Qin C., Zhong M., Huang X., Jia L., Li D.** // *Molec. Catal.* 2018. V. 459. P. 106-112. DOI: 10.1016/j.mcat.2018.08.002.
18. **Sadek R., Chalupka K.A., Mierczynski P., Rynkowski J., Millot Y., Valentin L., Casale S., Dzwigaj S.** // *Catal. Today.* 2020. V. 354. P. 109-122. DOI: 10.1016/j.cattod.2019.05.004.
19. **Beheshti M.S., Ahmadpour J., Behzad M., Arabi H.** // *Brazilian J. Chem. Eng.* 2021. V. 38. P. 101-121. DOI: 10.1007/s43153-020-00075-1.
20. **Fernandez S., Ostraat M. L., Zhang K.** // *AIChE J.* 2020. V. 66. N 9. P. e16943. DOI: 10.1002/aic.16943.
21. **Liu Q., Fan W.** // *Chem. J. Chinese Univ.* 2021. V. 42. N 1. P. 60-73.
22. **Jin Y., Zhang L., Liu J., Zhang S., Sun S., Asaoka S., Fujimoto K.** // *Micropor. Mesopor. Mater.* 2017. V. 248. P. 7-17. DOI: 10.1016/j.micromeso.2017.04.013.
23. **Verboekend D., Keller T.C., Milina M., Hauert R., Pérez-Ramírez J.** // *Chem. Mater.* 2013. V. 25. N 9. P. 1947-1959. DOI: 10.1021/cm4006103.
24. **Verboekend D., Pérez-Ramírez J.** // *Catal. Sci. Technol.* 2011. V. 1. N 6. P. 879-890. DOI: 10.1039/C1CY00150G.
25. **Sun H., Wang A., Sun K., Jiang J., Wang F., Gu Z.** // *J. Porous Mater.* 2019. V. 26. P. 961-970. DOI: 10.1007/s10934-018-0693-1.
26. **Zhang K., Fernandez S., Converse E.S., Kobaslija S.** // *Catal. Sci. Technol.* 2020. V. 10. N 14. P. 4602-4611. DOI: 10.1039/D0CY01209B.
27. **Link F., Ahad N., de Klerk A.** // *Am. Chem. Soc.* 2021. P. 311-352. DOI: 10.1021/bk-2021-1379.ch012.
28. **Chalupka K.A., Sadek R., Szkudlarek L., Mierczynski P., Maniukiewicz W., Rynkowski J., Gurgul J., Casale S., Brouri D., Dzwigaj S.** // *Res. Chem. Intermediates.* 2021. V. 47. P. 397-418. DOI: 10.1007/s11164-020-04343-0.
29. **Долуда В.Ю., Сульман М.Г., Матвеева В.Г., Лакина Н.В., Сульман Э.М.** // *Изв. вузов. Химия и хим. технология.* 2016. Т. 59. Вып. 2. С. 79-82. DOI: 10.6060/tcct.20165902.5268.

9. **Sineva L.V., Asalieva E.Y., Mordkovich V.Z.** // *Russ. Chem. Rev.* 2015.V. 84. N 11. P. 1176. DOI: 10.1070/RCR4464.

10. **Savost'yanov A.P., Narochnyi G.B., Yakovenko R.E., Saliev A.N., Sulima S.I., Zubkov I.N., Nekroenko, S.V., Mitchenko S.A.** // *Petrol. Chem.* 2017. V. 57. P. 1186-1189 (in Russian). DOI: 10.1134/S0965544117060251.
11. **Yakovenko R.E., Zubkov I.N., Bakun V.G., Agliullin M.R., Saliev A.N., Savost'yanov A.P.** // *Catal. Ind.* 2021. V. 13. P. 230-238. DOI: 10.1134/S2070050421030120.
12. **Yakovenko R.E., Savost'yanov A.P., Narochniy G.B., Soromotin V.N., Zubkov I.N., Papeta O.P., Svetogorov R.D., Mitchenko S.A.** // *Catal. Sci. Technol.* 2020. V. 10. N 22. P. 7613-7629. DOI: 10.1039/D0CY00975J.
13. **Sulima S.I., Bakun V.G., Yakovenko R.E., Shabel'skaya N.P., Saliev A.N., Narochnyi G.B., Savost'yanov A.P.** // *Kinet. Catal.* 2018. V. 59. P. 218-228. DOI: 10.1134/S0023158418020131.
14. **Abello S., Bonilla A., Perez-Ramirez J.** // *Appl. Catal. A: Gen.* 2009. V. 364. P. 191-198.
15. **Min J., Kim S., Kwak G., Kim Y.T., Han S.J., Lee Y., Jun K.W., Kim S.K.** // *Catal. Sci. Technol.* 2018. V. 8. N 24. P. 6346-6359. DOI: 10.1039/C8CY01931B.
16. **Tarach K., Góra-Marek K., Tekla J., Brylewska K., Datka J, Mlekodaj K., Makowski W., Igualada López M.C., Triguero J.M., Rey F.** // *J. Catal.* 2014. V. 312. P. 46-57. DOI: 10.1016/j.jcat.2014.01.009.
17. **Li H., Hou B., Wang J., Qin C., Zhong M., Huang X., Jia L., Li D.** // *Molec. Catal.* 2018. V. 459. P. 106-112. DOI: 10.1016/j.mcat.2018.08.002.
18. **Sadek R., Chalupka K.A., Mierczynski P., Rynkowski J., Millot Y., Valentin L., Casale S., Dzwigaj S.** // *Catal. Today.* 2020. V. 354. P. 109-122. DOI: 10.1016/j.cattod.2019.05.004.
19. **Beheshti M.S., Ahmadpour J., Behzad M., Arabi H.** // *Brazilian J. Chem. Eng.* 2021. V. 38. P. 101-121. DOI: 10.1007/s43153-020-00075-1.
20. **Fernandez S., Ostraat M. L., Zhang K.** // *AIChE J.* 2020. V. 66. N 9. P. e16943. DOI: 10.1002/aic.16943.
21. **Liu Q., Fan W.** // *Chem. J. Chinese Univ.* 2021. V. 42. N 1. P. 60-73.
22. **Jin Y., Zhang L., Liu J., Zhang S., Sun S., Asaoka S., Fujimoto K.** // *Micropor. Mesopor. Mater.* 2017. V. 248. P. 7-17. DOI: 10.1016/j.micromeso.2017.04.013.
23. **Verboekend D., Keller T.C., Milina M., Hauert R., Pérez-Ramírez J.** // *Chem. Mater.* 2013. V. 25. N 9. P. 1947-1959. DOI: 10.1021/cm4006103.
24. **Verboekend D., Pérez-Ramírez J.** // *Catal. Sci. Technol.* 2011. V. 1. N 6. P. 879-890. DOI: 10.1039/C1CY00150G.
25. **Sun H., Wang A., Sun K., Jiang J., Wang F., Gu Z.** // *J. Porous Mater.* 2019. V. 26. P. 961-970. DOI: 10.1007/s10934-018-0693-1.
26. **Zhang K., Fernandez S., Converse E.S., Kobaslija S.** // *Catal. Sci. Technol.* 2020. V. 10. N 14. P. 4602-4611. DOI: 10.1039/D0CY01209B.
27. **Link F., Ahad N., de Klerk A.** // *Am. Chem. Soc.* 2021. P. 311-352. DOI: 10.1021/bk-2021-1379.ch012.
28. **Chalupka K.A., Sadek R., Szkudlarek L., Mierczynski P., Maniukiewicz W., Rynkowski J., Gurgul J., Casale S., Brouri D., Dzwigaj S.** // *Res. Chem. Intermed.* 2021. V. 47. P. 397-418. DOI: 10.1007/s11164-020-04343-0.
29. **Doluda V.Yu., Sulman M.G., Matveeva V.G., Lakina N.V., Sulman E.M.** // *ChemChemTech [Izv. Vyssh. Uchebn. Zaved. Khim. Khim. Tekhnol.]*. 2016. V. 59. N 2. P. 79-82 (in Russian). DOI: 10.6060/tcct.20165902.5268.

30. **Степанов А.А., Коробицына Л.Л., Будаев Ж.Б., Восмериков А.В., Герасимов Е.Ю., Ишкильдина А.Х.** // *Изв. вузов. Химия и хим. технология.* 2023. Т. 66. Вып. 11. С. 58-66. DOI: 10.6060/ivkkt.20236611.7t.
31. **Verboekend D., Vilé G., Pérez-Ramírez J.** // *Cryst. Growth Des.* 2012. V. 12. N 6. P. 3123-3132. DOI: 10.1021/cg3003228.
32. **Guo X., Guo L., Zeng Y., Kosol R., Gao X., Yoneyama Y., Yang G., Tsubaki N.** // *Catal. Today.* 2021. V. 368. P. 196-203. DOI: 10.1016/j.cattod.2020.04.047.
33. **de Oliveira A.A., da Silva V., de Aguiar Pontes D., Almeida D.F., Silva D.S.A., Ferreira J.M., Santos R.S., Urquieta-Gonzalez E.A., Pontes L.A.M.** // *React. Kinet. Mech. Catal.* 2021. V. 132. P. 401-416. DOI: 10.1007/s11144-020-01921-6.
34. **Monama W., Mohiuddin E., Thangaraj B., Mdleleni M.M., Key D.** // *Catal. Today.* 2020. V. 342. P. 167-177. DOI: 10.1016/j.cattod.2019.02.061.
35. **Wijaya Y.P., Kristianto I., Lee H., Jae J.** // *Fuel.* 2016. V. 182. P. 588-596. DOI: 10.1016/j.fuel.2016.06.010.
36. **Wang Y., Sun Y., Lancelot C., Lamonier C., Morin J.C., Revel B., Rives A.** // *Micropor. Mesopor. Mater.* 2015. V. 206. P. 42-51. DOI: 10.1016/j.micromeso.2014.12.017.
37. **De la Osa, A.R., Romero A., Díez-Ramírez J., Valverde J.L., Sánchez P.** // *Top. Catal.* 2017. V. 60. P. 1082-1093. DOI: 10.1007/s11244-017-0792-2.
38. **Groen J.C., Abelló S., Villaescusa L.A., Pérez-Ramírez J.** // *Micropor. Mesopor. Mater.* 2008. V. 114. N 1-3. P. 93-102. DOI: 10.1016/j.micromeso.2007.12.025.
39. **Савостьянов А.П., Яковенко Р.Е., Нарочный Г.Б., Непомнящих Е.В., Митченко С.А.** // *Изв. вузов. Химия и хим. технология.* 2019. Т. 62. Вып. 8. С. 139-146. DOI: 10.6060/ivkkt.20196208.5905.
40. **Савостьянов А.П., Яковенко Р.Е., Нарочный Г.Б., Бакун В.Г., Сулима С.И., Якуба Э.С., Митченко С.А.** // *Кинетика и катализ.* 2017. Т. 58. Вып. 1. С. 86-97. DOI: 10.7868/S0453881117010075.
41. **Савостьянов А.П., Яковенко Р.Е., Нарочный Г.Б., Зубков И.Н., Сулима С.И., Соромотин В.Н., Митченко С.А.** // *Нефтехимия.* 2020. Т. 60. Вып. 1. С. 89-100. DOI: 10.31857/S0028242120010128.
42. **Нарочный, Г.Б., Яковенко Р.Е., Савостьянов А.П., Бакун В.Г.** // *Катализ в пром-сти.* 2016. Вып. 1. С. 37-42. DOI: 10.18412/1816-0387-2016-1-37-42.
43. **Яковенко Р.Е., Зубков И.Н., Савостьянов А.П., Соромотин В.Н., Краснякова Т.В., Папета О.П., Митченко С.А.** // *Кинетика и катализ.* 2021. Т. 62. Вып. 1. С. 109-119. DOI: 10.31857/S0453881121010159.
44. **Яковенко Р.Е, Зубков И.Н., Бакун В.Г., Папета О.П., Савостьянов А.П.** // *Нефтехимия.* 2022. Т. 62. Вып. 1. С. 119-131. DOI: 10.31857/S0028242122010063.
45. **Соромотин В.Н., Яковенко Р.Е., Лавренов С.А., Телегин Д.В., Митченко С.А.** // *Инж. Вестн. Дона.* 2022. Вып. 9. С. 1-11.
46. **Young R.A.** The Rietveld Method. Oxford: University Press. 1995. 298 p.
47. **Schanke D. Vada S., Blekkan E.A., Hilmen A., Hoff A., Holmen A.** // *J. Catal.* 1995. V. 156. N 1. P. 85-95. DOI: 10.1006/jcat.1995.1234.
48. **Xu D., Li W., Duan H., Ge Q., Xu H.** // *Catal. Lett.* 2005. V. 102. P. 229-235. DOI: 10.1007/s10562-005-5861-7.
49. **Lu T., Yan W., Xu R.** // *Inorg. Chem. Front.* 2019. V. 6. N 8. P. 1938-1951. DOI: 10.1039/C9QI00574A.

30. **Stepanov A.A., Korobitsyna L.L., Budaev Zh.B., Vosmerikov A.V., Gerasimov E.Yu., Ishkildina A.Kh.** // *ChemChemTech [Izv. Vyssh. Uchebn. Zaved. Khim. Khim. Tekhnol.]*. 2023. V. 66. N 11. P. 58-66 (in Russian). DOI: 10.6060/ivkkt.20236611.7t.
31. **Verboekend D., Vilé G., Pérez-Ramírez J.** // *Cryst. Growth Des.* 2012. V. 12. N 6. P. 3123-3132. DOI: 10.1021/cg3003228.
32. **Guo X., Guo L., Zeng Y., Kosol R., Gao X., Yoneyama Y., Yang G., Tsubaki N.** // *Catal. Today.* 2021. V. 368. P. 196-203. DOI: 10.1016/j.cattod.2020.04.047.
33. **de Oliveira A.A., da Silva V., de Aguiar Pontes D., Almeida D.F., Silva D.S.A., Ferreira J.M., Santos R.S., Urquieta-Gonzalez E.A., Pontes L.A.M.** // *React. Kinet. Mech. Catal.* 2021. V. 132. P. 401-416. DOI: 10.1007/s11144-020-01921-6.
34. **Monama W., Mohiuddin E., Thangaraj B., Mdleleni M.M., Key D.** // *Catal. Today.* 2020. V. 342. P. 167-177. DOI: 10.1016/j.cattod.2019.02.061.
35. **Wijaya Y.P., Kristianto I., Lee H., Jae J.** // *Fuel.* 2016. V. 182. P. 588-596. DOI: 10.1016/j.fuel.2016.06.010.
36. **Wang Y., Sun Y., Lancelot C., Lamonier C., Morin J.C., Revel B., Rives A.** // *Micropor. Mesopor. Mater.* 2015. V. 206. P. 42-51. DOI: 10.1016/j.micromeso.2014.12.017.
37. **De la Osa, A.R., Romero A., Díez-Ramírez J., Valverde J.L., Sánchez P.** // *Top. Catal.* 2017. V. 60. P. 1082-1093. DOI: 10.1007/s11244-017-0792-2.
38. **Groen J.C., Abelló S., Villaescusa L.A., Pérez-Ramírez J.** // *Micropor. Mesopor. Mater.* 2008. V. 114. N 1-3. P. 93-102. DOI: 10.1016/j.micromeso.2007.12.025.
39. **Savostyanov A.P., Yakovenko R.E., Narochny G.B., Nepomnyashchikh E.V., Mitchenko S.A.** // *ChemChemTech [Izv. Vyssh. Uchebn. Zaved. Khim. Khim. Tekhnol.]*. 2019. V. 62. N 8. P. 139-146 (in Russian). DOI: 10.6060/ivkkt.20196208.5905.
40. **Savost'yanov A.P., Yakovenko R.E., Narochnyi G.B., Bakun V.G., Sulima S.I., Yakuba E.S., Mitchenko S.A.** // *Kinet. Catal.* 2017. V. 58. P. 81-91. DOI: 10.1134/S0023158417010062.
41. **Savost'yanov A.P., Yakovenko R.E., Narochnyi G.B., Zubkov I.N., Sulima S.I., Soromotin V.N., Mitchenko S.A.** // *Petrol. Chem.* 2020. V. 60. P. 81-91. DOI: 10.1134/S0023158418020131.
42. **Narochny G.B., Yakovenko R.E., Savostianov A.P., Bakun V.G.** // *Katal. Promysh.* 2016. V. 16. N 1. P. 37-42 (in Russian). DOI: 10.18412/1816-0387-2016-1-37-42.
43. **Yakovenko R.E., Zubkov I.N., Savost'yanov A.P., Soromotin V.N., Krasnyakova T.V., Papeta O.P., Mitchenko S.A.** // *Kinet. Catal.* 2021. V. 62. P. 172-180. DOI: 10.1134/S0023158421010122.
44. **Yakovenko R.E., Zubkov I.N., Bakun V.G., Papeta O.P., Savostyanov A.P.** // *Petrol. Chem.* 2022. V. 62. P. 101-111. DOI: 10.1134/S0965544122010157.
45. **Soromotin V.N., Yakovenko R.E., Lavrenov S.A., Telegin D.V., Mitchenko S.A.** // *Inzh. Vestn. Dona.* 2022. P. 1-11 (in Russian).
46. **Young R.A.** The Rietveld Method. Oxford: University Press. 1995. 298 p.
47. **Schanke D. Vada S., Blekkan E.A., Hilmen A., Hoff A., Holmen A.** // *J. Catal.* 1995. V. 156. N 1. P. 85-95. DOI: 10.1006/jcat.1995.1234.
48. **Xu D., Li W., Duan H., Ge Q., Xu H.** // *Catal. Lett.* 2005. V. 102. P. 229-235. DOI: 10.1007/s10562-005-5861-7.
49. **Lu T., Yan W., Xu R.** // *Inorg. Chem. Front.* 2019. V. 6. N 8. P. 1938-1951. DOI: 10.1039/C9QI00574A.

50. **Do Nascimento A.R., De Figueredo G.P., Silva E.M.F., Melo M.A.F., Melo D.M.A., De Souza M.J.B.** // *Rev. Virtual Quim.* 2017. V. 9. N 4. P. 1570-1582. DOI: 10.21577/1984-6835.20170092.
51. **Groen J.C., Moulijn J.A., Pérez-Ramírez J.** // *J. Mater. Chem.* 2006. V. 16. N 22. P. 2121-2131. DOI: 10.1039/B517510K.
52. **Groen J.C., Peffer L.A., Moulijn J.A., Pérez-Ramírez J.** // *Chem.–A Eur. J.* 2005. V. 11. N 17. P. 4983-4994. DOI: 10.1002/chem.200500045.
53. **Breck D.** Zeolite molecular sieves. 1976. New York: Wiley. 771 p.
54. **Pelmenschikov A.G., Morosi G., Gamba A.** // *J. Phys. Chem.* 1992. V. 96. N 5. P. 2241-2246. DOI: 10.1021/j100184a040.
55. **Olson D.H., Haag W.O., Borghard W.S.** // *Micropor. Mesopor. Mater.* 2000. V. 35. P. 435-446. DOI: 10.1016/S1387-1811(99)00240-1.
56. **Brazovskaya E.Y., Golubeva O.Y.** // *Glass Phys. Chem.* 2021. V. 47. N 6. P. 726-730. DOI: 10.1134/S108765962106002X.
57. **Guo P., Yan N., Wang L., Zou X.** // *Cryst. Growth Des.* 2017. V. 17. N 12. P. 6821-6835. DOI: 10.1021/acs.cgd.7b01410.
58. **Akhmedov V.M., Al-Khowaiter S.H.** // *Catal. Rev.* 2007. V. 49. N 1. P. 33-139. DOI: 10.1080/01614940601128427.
59. **Hao W., Zhang W., Guo Z., Ma J., Li R.** // *Catalysts*. 2018. V. 8. N 11. P. 504. DOI: 10.3390/catal8110504.
60. **Mathieu R., Vieillard P.** // *Micropor. Mesopor. Mater.* 2010. V. 132. N 3. P. 335-351. DOI: 10.1016/j.micromeso.2010.03.011.
61. **Cheng K., Kang J., Huang S., You Z., Zhang Q., Ding J., Hua W., Deng J., Wang Y.** // *ACS Catal.* 2012. V. 2. N 3. P. 441-449. DOI: 10.1021/cs200670j.
62. **Wang F., Zheng Y., Huang Y., Yang X., Xu G., Kang J., Liu C., Zheng Z.** // *J. Analyt. Appl. Pyrol.* 2017. V. 126. P. 180-187. DOI: 10.1016/j.jaap.2017.06.010.
63. **Murzin D.Y.** // *Kinet. Catal.* 2020. V. 61. P. 80-92. DOI: 10.1134/S0023158420010073.
64. **Kokuryo S., Miyake K., Uchida Y., Mizusawa A., Kubo T., Nishiyama N.** // *Mater. Today Sustainability*. 2022. V. 17. P. 100098. DOI: 10.1016/j.mtsust.2021.100098.
65. **Bulavchenko O.A., Vinokurov Z.S.** // *Catalysts*. 2023. V. 13. N 11. P. 1421. DOI: 10.3390/catal13111421.
66. **Горшков А.С., Синева Л.В., Грязнов К.О., Митберг Э.Б., Мордкович В.З.** // *Изв. вузов. Химия и хим. технология.* 2022. Т. 65. Вып. 11. С. 65-70. DOI: 10.6060/ivkkt.20226511.2y.

50. **Do Nascimento A.R., De Figueredo G.P., Silva E.M.F., Melo M.A.F., Melo D.M.A., De Souza M.J.B.** // *Rev. Virtual Quim.* 2017. V. 9. N 4. P. 1570-1582. DOI: 10.21577/1984-6835.20170092.
51. **Groen J.C., Moulijn J.A., Pérez-Ramírez J.** // *J. Mater. Chem.* 2006. V. 16. N 22. P. 2121-2131. DOI: 10.1039/B517510K.
52. **Groen J.C., Peffer L.A., Moulijn J.A., Pérez-Ramírez J.** // *Chem.–A Eur. J.* 2005. V. 11. N 17. P. 4983-4994. DOI: 10.1002/chem.200500045.
53. **Breck D.** Zeolite molecular sieves. 1976. New York: Wiley. 771 p.
54. **Pelmenschikov A.G., Morosi G., Gamba A.** // *J. Phys. Chem.* 1992. V. 96. N 5. P. 2241-2246. DOI: 10.1021/j100184a040.
55. **Olson D.H., Haag W.O., Borghard W.S.** // *Micropor. Mesopor. Mater.* 2000. V. 35. P. 435-446. DOI: 10.1016/S1387-1811(99)00240-1.
56. **Brazovskaya E.Y., Golubeva O.Y.** // *Glass Phys. Chem.* 2021. V. 47. N 6. P. 726-730. DOI: 10.1134/S108765962106002X.
57. **Guo P., Yan N., Wang L., Zou X.** // *Cryst. Growth Des.* 2017. V. 17. N 12. P. 6821-6835. DOI: 10.1021/acs.cgd.7b01410.
58. **Akhmedov V.M., Al-Khowaiter S.H.** // *Catal. Rev.* 2007. V. 49. N 1. P. 33-139. DOI: 10.1080/01614940601128427.
59. **Hao W., Zhang W., Guo Z., Ma J., Li R.** // *Catalysts*. 2018. V. 8. N 11. P. 504. DOI: 10.3390/catal8110504.
60. **Mathieu R., Vieillard P.** // *Micropor. Mesopor. Mater.* 2010. V. 132. N 3. P. 335-351. DOI: 10.1016/j.micromeso.2010.03.011.
61. **Cheng K., Kang J., Huang S., You Z., Zhang Q., Ding J., Hua W., Deng J., Wang Y.** // *ACS Catal.* 2012. V. 2. N 3. P. 441-449. DOI: 10.1021/cs200670j.

62. **Wang F., Zheng Y., Huang Y., Yang X., Xu G., Kang J., Liu C., Zheng Z.** // *J. Analyt. Appl. Pyrol.* 2017. V. 126. P. 180-187. DOI: 10.1016/j.jaap.2017.06.010.

63. **Murzin D.Y.** // *Kinet. Catal.* 2020. V. 61. P. 80-92. DOI: 10.1134/S0023158420010073.
64. **Kokuryo S., Miyake K., Uchida Y., Mizusawa A., Kubo T., Nishiyama N.** // *Mater. Today Sustainability.* 2022. V. 17. P. 100098. DOI: 10.1016/j.mtsust.2021.100098.
65. **Bulavchenko O.A., Vinokurov Z.S.** // *Catalysts*. 2023. V. 13. N 11. P. 1421. DOI: 10.3390/catal13111421.

66. **Gorshkov A.S., Sineva L.V., Gryaznov K.O., Mitberg E.B., Mordkovich V.Z.** // *ChemChemTech [Izv. Vyssh. Uchebn. Zaved. Khim. Khim. Tekhnol.]*. 2022. V. 65. N 11. P. 65-70. DOI: 10.6060/ivkkt.20226511.2y.

Поступила в редакцию 29.12.2023
Принята к опубликованию 12.03.2024

Received 29.12.2023
Accepted 12.03.2024